Published OnlineFirst May 10, 2013; DOI: 10.1158/1541-7786.MCR-12-0177

Cell Death and Survival

Molecular Cancer Research

Development of a Novel Class of Tubulin Inhibitors with Promising Anticancer Activities

Jingle Xi[1,3,5], Xuejun Zhu[4,6], Yongmei Feng[4], Na Huang[5], Guifen Luo[1,3], Yongjun Mao[1,3], Xiaofeng Han[1,3], Wang Tian[1,3], Guirong Wang[2,3], Xiaobing Han[1,3], Rongcheng Luo[5], Ziwei Huang[1,3], and Jing An[1,3]

Abstract

We have developed a novel class (2-amino-4-phenyl-4H-chromene-3-carboxylate) of inhibitors of tubulin assembly by modifying HA14-1, which is a Bcl-2 inhibitor discovered by our group. Three of these compounds, mHA1, mHA6, and mHA11, showed *in vitro* cytotoxicities against tumor cells that were more potent and more stable than the backbone compound HA14-1, with nM IC_{50} values. In contrast, the cytotoxic effects of these compounds on normal cells were minimal. Computational docking, colchicine-tubulin competitive binding, and tubulin polymerization studies demonstrated that these compounds bind at the colchicine-binding site on tubulin and inhibit the formation of microtubules. Treatment of HL-60/Bcl-2 leukemia and CRL5908 lung cancer cells with these mHA compounds led to pronounced microtubule density decreases, G2/M cell cycle arrest, and apoptosis, as determined by immunofluorescence microscopy, flow cytometry, and DNA fragmentation analysis. Combined, these data identify a novel class of compounds that inhibit tubulin assembly and limit cancer cell phenotypes.

Implications: This study supports the continued development of novel anti-tubulin assembly inhibitors as potential anticancer agents. *Mol Cancer Res; 11(8); 856–64. ©2013 AACR.*

Introduction

Microtubules are components of cytoskeleton and are composed of α- and β-tubulin that form heterodimers (1). Microtubules are involved in many cellular processes, including intracellular transport, maintenance of cell shape, polarity, cell signaling, mitosis, and cytokinesis (2). Their role in mitosis makes them important cellular targets for anticancer drug developments. In the eukaryotic cell cycle, tubulin is polymerized into microtubules, which form the mitotic spindle. The spindle then moves the chromosomes to the opposite sides of the cell, in preparation for cell division into 2 daughter cells. Because of this important role in cell proliferation, microtubules have been recognized as one of the successful and efficacious drug targets for the development of novel anticancer chemotherapeutics (3–7).

Microtubule-inhibiting agents (MIA) currently used in clinic therapies work through the suppression of the microtubule dynamics by misdirecting the formation of a functional mitotic spindle in fast-dividing tumor cells. This arrests the cells in G_2–M phase, thereby leading to apoptosis of the tumor cells. Based on their mechanism of action, MIAs are classified into 2 broad categories: microtubule stabilizing agents and destabilizing agents. Most MIAs bind to 1 of 3 sites on tubulin, the colchicine site, the vinblastine site, or the paclitaxel site (8). Because of the potent anticancer activity, these apoptotic therapeutic agents that target microtubules are among the most commonly prescribed antitumor agents. However, as with other anticancer drugs, intolerable toxicities and the emergence of drug resistance have limited the clinical use of the drugs targeting microtubules (9–11). Therefore, a need still exists for discovery and development of novel chemotherapeutic agents that target microtubules, but that show lower drug resistance and fewer toxic side effects.

We have been focusing our efforts for many years on the research and development of novel tumor therapeutic agents that target different factors involved in apoptotic pathways. The small compound dubbed HA14-1, identified by our group, was the first reported Bcl-2 inhibitor (12, 13). In subsequent studies, we found that it can also bind tubulin in a manner that is competitive with colchicine, which binds at the interface within α/β-tubulin heterodimers. Colchicine is now a branded drug for treating several clinical diseases, including gout and Familial Mediterranean fever. Although the effectiveness and side effects of colchicine in cancer treatment need to be further characterized, the colchicine-binding site is a potential drug target that has attracted much attention for development of new anticancer agents (14); several such compounds are undergoing clinical trials (8, 15). In this study, we used HA14-1 as the initial template

Authors' Affiliations: Departments of [1]Pharmacology and [2]Surgery; [3]Upstate Cancer Research Institute, SUNY Upstate Medical University, Syracuse, New York; [4]Sanford-Burnham Medical Research Institute, La Jolla, California; [5]Department of Oncology, Nanfang Hospital, Southern Medical University, Guangzhou; and [6]Department of Production & Operation, China National Agrochemical Corporation, Beijing, China

J. Xi and X. Zhu contributed equally to the article.

Corresponding Authors: Jing An, Department of Pharmacology, SUNY Upstate Cancer Research Institute, State University of New York, 750 East Adams Street, Syracuse, NY 13210. Phone: 315-464-7952; Fax: 315-464-8014; E-mail: anji@upstate.edu; Ziwei Huang, huangz@upstate.edu; and Rongcheng Luo, luorc01@163.com

doi: 10.1158/1541-7786.MCR-12-0177

Published OnlineFirst May 10, 2013; DOI: 10.1158/1541-7786.MCR-12-0177

compound and developed a new class (2-amino-4-phenyl-4H-chromene-3-carboxylate) of novel microtubule-targeting agents that show promising antitumor activities.

Materials and Methods

Chemical synthesis

A general synthetic procedure of mHA1, mHA6, and mHA11 is illustrated in Fig. 1. These compounds were synthesized using a one-pot 3-component reaction of substituted benzaldehyde, phenol analogs, and ethyl cyanoacetate in the presence of piperidine. All of the new compounds described were characterized by ^{1}H NMR and mass spectrometry spectra.

Preparation of mHA1

A mixture of 3-bromo-4,5-dimethoxybenzaldehyde (0.49 g, 0.002 mol), 3-(dimethylamino) phenol (0.27 g, 0.002 mol), ethyl cyanoacetate (0.21 mL, 0.002 mol), and piperidine (0.4 mL, 0.004 mol) was suspended in 15 mL anhydrous ethanol and stirred at room temperature for 4 hours. After diluting with 80 mLCH_2Cl_2 and washing with water, the organic layer was dried over Na_2SO_4. The Na_2SO_4 was then removed by filtration and the solvent was evaporated. The crude product was purified by column chromatography (hexane/CH_2Cl_2) to give 0.6 g mHA1 at 63% yield.

Preparation of mHA6

Starting from 3-bromo-4,5-dimethoxybenzaldehyde, naphthalen-1-ol, and ethyl cyanoacetate, we then followed the procedure for the synthesis of mHA1, to give 0.45 g (46% yield) of mHA6.

Preparation of mHA11

Starting from 3-chlorobenzaldehyde, 3-(dimethylamino) phenol, and ethyl cyanoacetate, we then followed the procedure for the synthesis of mHA1, to give 0.32 g (43% yield) of mHA11.

Cell culture

The human leukemic HL-60/Bcl-2 cell line was obtained from Dr. Kapil N. Bhalla (University of Miami School of Medicine, Miami, FL; ref. 13), which has been stably transfected with pZip-Bcl-2 plasmid. CRL5908 lung cancer cell line was kindly provided by Dr. Sandra G. Hudson. Cells were cultured in RPMI 1640 medium supplemented with 10% FBS, 2 mmol/L glutamine, 100 U/mL penicillin, 100 μg/mL streptomycin, and 800 μg/mL genticin (G418; Invitrogen). Cells were maintained in a humidified 5% CO_2 atmosphere at 37°C.

Human bone marrow specimen collection

Human bone marrow specimens were obtained from three healthy adult donors. The patients were placed in the lateral decubitus position, with the top leg flexed and the lower leg straight. After sterilizing the chosen area of the posterior iliac crest skin, 10 mL of 1% lidocaine was infiltrated into the skin and subcutaneous tissue to anesthetize an area approximately

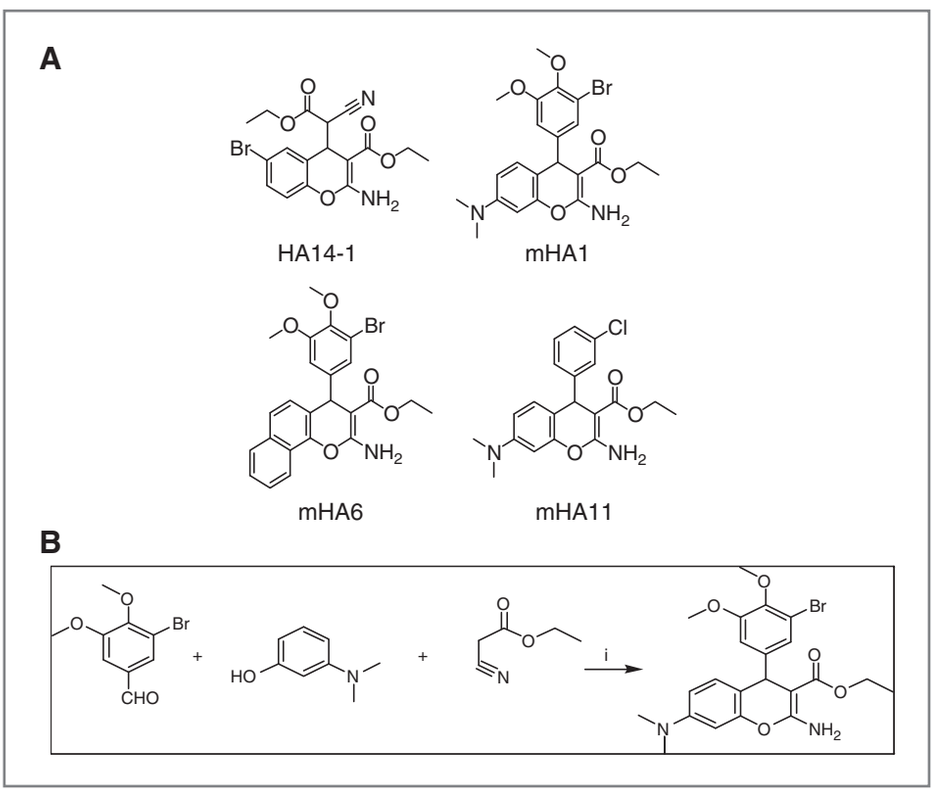

Figure 1. Structures of HA14-1 and its analogs mHA1, mHA6, and mHA11 (A); and one-pot reaction for the synthesis of mHA1, mHA6, and mHA11 (B).

Published OnlineFirst May 10, 2013; DOI: 10.1158/1541-7786.MCR-12-0177

2 to 3 cm in diameter. An incision was made in the skin with a small surgical blade, through which the bone marrow aspiration needle, with a stylet locked in place, was inserted. Once the needle contacted the bone, it was advanced by slowly rotating clockwise and counterclockwise until the cortical bone was penetrated and the marrow cavity was entered. Once within the marrow cavity, the stylet was removed. Approximately, 1 mL of bone marrow was aspirated using a 10 mL syringe. The sample was then transferred into an anticoagulant-containing (heparin) tube. The marrow needle was removed, and pressure was applied to the aspiration site with gauze until any bleeding had stopped. The bone marrow specimen was then carefully diluted with 4 mL medium and layered over 5 mL Ficoll-Paque PLUS (GE Healthcare) in a tube, without disturbing the interface, and centrifuged at 3,000 rpm for 30 minutes. The interface layer was aspirated to another tube, washed with medium, and incubated with mHA1, mHA6, or mHA11 at different concentrations (as described later) for 72 hours.

Measurement of cell viability

The cytotoxic effects of the HA14-1 analogs were measured by plating 3×10^4 cells/well in 96-well plates and determining cell survival. Cells were treated with various concentrations of these compounds (0.1–3 μmol/L). The samples were then incubated at 37°C for 72 hours in a 5% CO_2 and 95% humidity incubator. After incubation, cell viability was measured using a CellTiter-Blue assay kit (Promega) according to the manufacturer's instructions. Briefly, 20 μL of CellTiter-Blue reagent was added to 100 μL of culture media and cells were incubated for 2 to 4 hours at 37°C. Afterward, fluorescence at $540_{Ex}/600_{Em}$ was measured using a fluorescence plate reader (BioTek, Synergy 2). Each experimental data point was generated from at least 3 independent experiments.

Cell morphological change

Cells were treated with mHAs at 1 μmol/L of mHAs for 24 hours and then examined for morphological changes by inverted fluorescence microscopy and photography.

Cell-cycle analysis

HL-60/Bcl-2 cells (1×10^6) were treated with 1, 3, and 5 μmol/L of mHA1, mHA6, mHA11, respectively, for 24 hours at 37°C. Cells were harvested at 1,100 rpm and washed twice with PBS, then resuspended in 100 μL of PBS and 1 mL of 75% cold ethanol and stored at −20°C overnight. After centrifugation at 1,100 rpm for 5 minutes, the supernatant was removed. A 500 μL PI staining buffer containing 80 μg/mL of propidium iodide, 100 μg/mL of RNAse A, and 1% Triton was added to the samples. The cells were incubated for at least half an hour and then analyzed by flow cytometry with a FACScalibur system (LSRII; Becton Dickinson) using FlowJo7.5 analysis software.

DNA fragmentation analysis

HL-60/Bcl-2 cells were resuspended in fresh medium and added to 24-well plate wells at a density of 1×10^6 cells/well, in a final volume of 1 mL. Vehicle control (DMSO), positive control (colchicine at 0.1 and 1 μmol/L), and mHA1, mHA6, or mHA11 (at 1 and 5 μmol/L) compounds were then added to the appropriate wells. The plate was incubated for 24 hours, and total DNA was extracted from the cells in each well using an apoptotic DNA-ladder kit following the manufacturer's instructions (Qiagen). The DNA samples were subjected to 2% agarose gel electrophoresis and visualized with ethidium bromide staining.

Tubulin polymerization assay

Tubulin polymerization assays were conducted using the polymerization assay kit following the manufacturer's instructions (Cytoskeleton, Inc.). Briefly, 50 μL of 3 mg/mL tubulin (>99% pure) proteins in G-PEM buffer (80 mmol/L PIPES, pH 6.9, 2 mmol/L $MgCl_2$, 0.5 mmol/L EGTA, 1 mmol/L GTP, and 15% glycerol) was placed in 96-well microtiter plates in the presence of test agents. Polymerization was measured at every 60 seconds intervals for 1 hour using a Synergy 2 microplate reader (BioTek; excitation at 360 nm and emission at 420 nm) at 37°C. Tubulin levels were normalized to a value of 100 for the vehicle control.

[^{3}H]Colchicine–tubulin binding assay

One micromolar radiolabeled colchicine [ring C, Methoxy-^{3}H] (Perkin-Elmer; 1 mCi/mL), 1% DMSO and various concentrations of test compounds in 50 μL G-PEM buffer containing 80 mmol/L PIPES (pH 6.8), 1 mmol/L EGTA, 1 mmol/L $MgCl_2$ and 1 mmol/L GTP, and 5% glycerol were incubated with 1 μmol/L tubulin (>99% pure; Cytoskeleton, Inc.; 0.2 mg/mL) at 37°C for 60 minutes. The binding solutions were filtered through a stack of 2 DEAE-cellulose filters and washed twice. The radioactivity in the filtrates was determined by liquid scintillation spectrometry (Perkin-Elmer Wallac). Nonlinear regression was used to analyze the data using GraphPad Prism.

Immunolfluorescence staining

After treatment with 1 μmol/L of mHA1, mHA6, and mHA11 for 24 hours, the densities of microtubule and actin in adherent CRL5908 lung cancer cells were evaluated using immunobiochemistry. CRL 5908 cells at 5×10^4 per well were cultured as described previously. One day after seeding, 1 μmol/L mHA1, mHA6, or mHA11 were added to the cells and cultured at 37°C for 24 hours. Thereafter, cells were fixed for 30 minutes at 4°C in 4% paraformaldehyde and incubated with 0.1% Triton X-100 permeabilizing buffer for 15 minutes at room temperature. After washing with PBS and blocking with 2% BSA in PBS for 30 minutes at room temperature, cells were incubated for 1 hour protected from light at room temperature in 1:2,000 anti–α-tubulin monoclonal antibody (Sigma) and 7:1,000 Rhodamine–Phalloidin-labeled anti-actin antibody (Cytoskeleton) in PBS. Cells were then washed with PBS and incubated for 30 minutes protected from light at room temperature with 1:200 fluorescein isothiocyanate–labeled antimouse IgG antibody (Sigma) in PBS. Subsequently, all cells were stained with 1 μg/mL 4′,6-diamidino-2-phenyl-indole (Sigma). Samples

Published OnlineFirst May 10, 2013; DOI: 10.1158/1541-7786.MCR-12-0177

were examined under a fluorescence microscope (Eclipse TE2000-U; Nikon) and photographed using a digital camera equipped with a fluorescein figure analysis system (NIS-Elements F3.0; Nikon).

Molecular modeling

The crystal structure of α/β-tubulin heterodimers in a complex with DAMA-colchicine (PDB reference: 1SA0; ref. 16) was used to predict the binding models of tubulin bind with designed compounds. The binding modes of designed ligands 1, 6, 11 with tubulin were predicted by using the Autodock4 program. In preparation of receptor grid files, a 60 × 55 × 60 grid with a grid spacing of 0.375 Å was defined to cover the interface of α/β-tubulin heterodimer. Grid maps were then generated by Autogrid4 for docking simulations. Lamarkian genetic algorithm was adopted in Autodock4 calculation, and 100 runs were conducted for each ligand. The whole receptor structure was set to be rigid during the simulations. All other parameters for Autogrid and Autodock calculations were set to default values in AutoDockTools-1.5.2. For each ligand, the 100 conformations resulted from Autodock simulations were clustered and the representative binding mode to tubulin with lowest predicted binding free energy.

Statistical analysis

Average values were expressed as mean ± SD. *P*-values were calculated by one-way ANOVA (PSIPLOT).

Results

Cytotoxicity of new mHA agents toward leukemic HL-60/Bcl-2 cells and normal human bone marrow cells

Of the series of HA14-1 analogs synthesized, mHA1, mHA6, and mHA11, showed the best antitumor activity. Human leukemia HL-60/Bcl-2 cells were treated with different concentrations of mHA1, mHA6, and mHA11 (0.1–3 μmol/L) for 72 hours. Cell viability, assessed by the CellTiter-Blue Cell Viability Assay, showed that the effects of mHA1, mHA6, and mHA11 were dose dependent, with IC_{50} values of 0.932 ± 0.128, 0.958 ± 0.045, and 0.648 ± 0.049 μmol/L, respectively (Fig. 2A–C), whereas IC_{50} of the parent compound, HA14-1, was 9.394 ± 0.18 μmol/L (data not shown). Overall, these HA14-1 analogs were much more potent than the parent HA14-1 compound.

The usefulness of a potential anticancer compound depends not only on its cytotoxicity in malignant cells, but also on its relative lack of toxicity toward normal tissues. We therefore evaluated the effects of the HA14-1 analogs on normal human bone marrow cells (HBMC). These cells were obtained from 3 normal adult donors, as previously described. After exposure to mHA1, mHA6, or mHA11 at different concentrations (0.1–3 μmol/L) for 72 hours, cell viability was assessed by the CellTiter-Blue Cell Viability Assay. As shown in Fig. 2A–C, these compounds had almost no effects on normal HBMCs below 3 μmol/L concentration, whereas 3 μmol/L mHAs were able to kill almost all of the malignant HL-60/Bcl-2 cells ($P < 0.01$). In contrast,

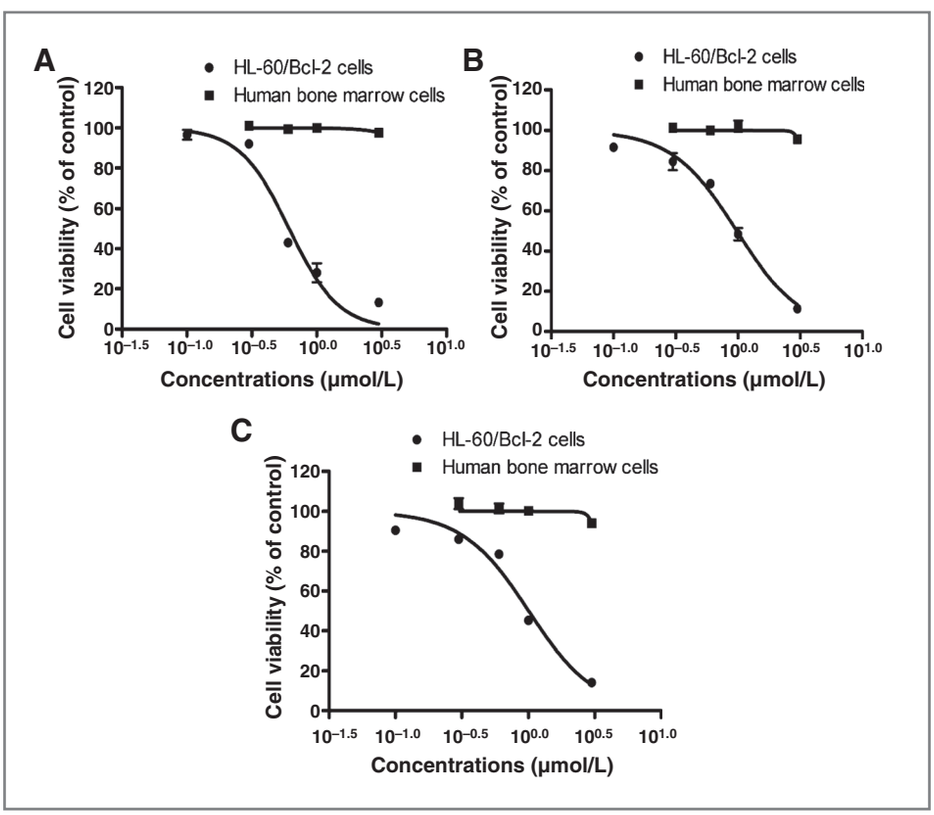

Figure 2. A–C, cytotoxicity of mHA toward HL-60/Bcl-2 cell lines and normal HBMCs. Cells were treated with different concentrations of mHA (A, mHA1; B, mHA6; C, mHA11) for 72 hours, as described in the text. Cell viability was then evaluated with a CellTiter-Blue assay. Viability at each concentration was expressed as a percentage of the viability compared to the vehicle (DMSO) control. The experiments were done three times and data were analyzed in Microsoft Excel and plotted in Prism 5.

Published OnlineFirst May 10, 2013; DOI: 10.1158/1541-7786.MCR-12-0177

treatment with colchicine, used here as the control colchicine site drug, resulted in the death of 30% of normal HBMCs at 25 nmol/L (data not shown), even though its IC_{50} was only 33.5 ± 3.5 nmol/L on HL-60/Bcl-2 cells. The high toxicity of colchicine against normal cells limited its therapeutic value on cancer.

Cell morphology changes in response to mHAs

HL-60/Bcl-2 cells are suspension cells and typically have a spherical shape. After treatment with 1 μmol/L of mHAs for 24 hours, morphological changes including cell elongation, asymmetry, and formation of long pseudopodia were observed by fluorescence microscope (Fig. 3A).

DNA fragmentation analysis

To confirm that these compounds could induce apoptosis in HL-60/Bcl-2 cells, we conducted DNA fragmentation analysis, which is a key feature of apoptosis (17). A clear DNA ladder was observed after 24-hour treatment with 1 or 5 μmol/L mHA1, mHA6, or mHA11 and 0.1 or 1 μmol/L of colchicine, indicating that colchicine, and mHA1, mHA6, and mHA11 could induce apoptotic cell death in HL-60/Bcl-2 cells (Fig. 3B).

G_2–M cell-cycle arrest caused by mHAs

To determine whether the inhibition of growth due to HA14-1 analogs is associated with cell-cycle perturbation, the distribution of cells in different phases of the cell cycle was determined by flow cytometry, and analyzed using FlowJo7.5 analysis software. The HL-60/Bcl-2 control cell population profile is shown in Table 1 and indicates that most of the cells were in the G_1- and S-phase. The HA14-1 analogs all caused a statistically significant increase in the G_2–M cell population. For example, increased from 14.5% to 70.9%, 55.8%, and 54.7% were observed for mHA1, mHA6, and mHA11 treatments, respectively, when administered at 1 μmol/L for 24 hours. A concomitant decrease in G_1 and S cell population was observed. The distribution of cells in different phases of the cell cycle is summarized in Table 1. After exposure, HL-60/Bcl-2 leukemia cells to 1, 3, and 5 μmol/L of mHA1, mHA6, and mHA11, a subdiploid peak was observed (Table 1). An increase in the sub-G_0/G_1 cell population from 5% to 13.3%, 13.9% to 20.3%, and 16.7% to 28.3% was occurred when cells were treated with 1 to 5 μmol/L mHA1, mHA6, and mHA11, respectively, for 24 hours.

Table 1. Summary of the distribution of cells in different phases of the cell cycle

Name	Concentration (μmol/L)	Cell cycle			
		Sub-G_1	G_1	S	G_2–M
	Control	0.3	39.3	44.5	14.5
mHA1	1	5	5.9	6.9	70.9
	3	12	6	10.2	62.9
	5	13.3	8.6	17.3	56.1
mHA6	1	13.9	10	15	55.8
	3	16.4	11.8	21.2	45.3
	5	20.3	13.2	27.3	37.7
mHA11	1	16.7	10.7	14.8	54.4
	3	18.4	7.3	12.7	57.8
	5	28.3	13.7	22.3	33.7

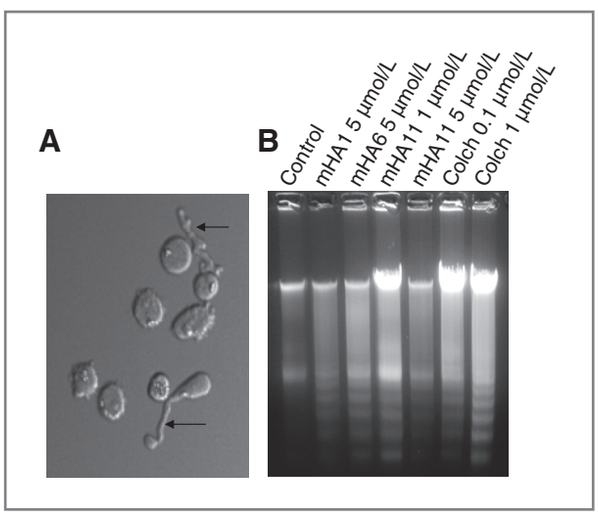

Figure 3. A, morphological changes of HL-60/Bcl-2 cells in response to treatment with mHA1, mHA6, and mHA11. Cells were treated with 1 μmol/L mHAs for 24 hours and then examined using a fluorescence microscope. Most of the cells lost their normal spherical shape and morphological changes including cell elongation, asymmetry, and formation of long pseudopodia could be observed (A). Magnification is 200×. The result was representative of three independent experiments. B, induction of DNA fragmentation. HL-60/Bcl-2 cells were treated for 24 hours with mHA1, mHA6, mHA11 (1 or 5 μmol/L), or colchicine (Colch, 0.1 or 1 μmol/L). The DNA ladder was detected as described in "Materials and Methods."

All mHAs bind to colchicine-binding site and inhibit tubulin polymerization

In the crystal structure of α/β-tubulin heterodimers complex with DAMA-colchicine, colchicine binds at the interface of α/β-tubulin heterodimer and inhibits the assembly of tubulin by preventing curved tubulin from adopting a straight structure. The result of our docking study shows that mHA1, mHA6, and mHA11 could bind at the same site of colchicine on the tubulin protein. Radioligand binding assay confirms dose-dependent inhibition of tubulin polymerization by competing with the [^{3}H]colchicine binding to tubulin for these 3 mHAs (Fig. 4). To investigate the inhibitory effects of mHA1, mHA6, and mHA11 on tubulin polymerization, >99% pure tubulin was treated with each of these compounds at 0.25 to 5 μmol/L for 1-hour at 37°C (Fig. 5). The contents of polymerized microtubules were measured every 60 seconds for 1 hour using 360 nm excitation and 420 nm emission filters. Results showed that mHA1, mHA6, and mHA11 exhibited strong inhibition of the microtubule formation comparable to the known microtubule polymerization inhibitor colchicine (IC_{50} = 25 nmol/L), with IC_{50} values of 669, 730, and 755 nmol/L, respectively.

Published OnlineFirst May 10, 2013; DOI: 10.1158/1541-7786.MCR-12-0177

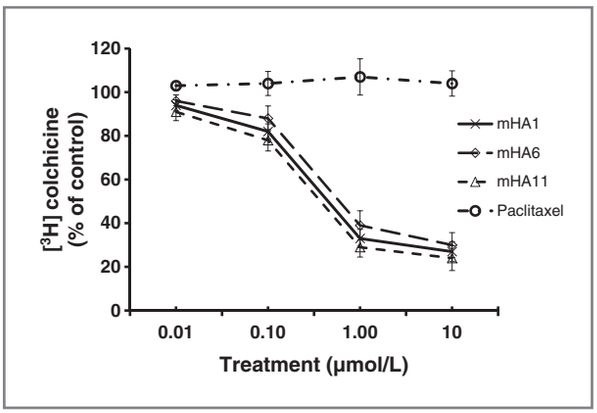

Figure 4. Effect of mHA1, mHA6, and mHA11 on tubulin binding of [^{3}H]colchicine. Tubulin (>99% pure) was incubated with tritiated tubulin binders in the presence of mHA1 (x), mHA6 (◇), mHA11 (Δ), or Paclitaxel (○) at indicated concentrations for 1 hour at 37°C. Each point represents the mean of three independent experiments, and error bars indicate the standard error.

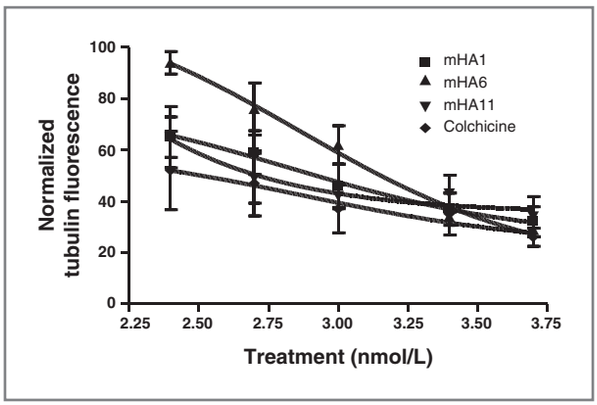

Figure 5. Inhibition of *in vitro* polymerization of tubulin using mHA1, mHA6, or mHA11. The steady-state tubulin assembly level in the absence of an inhibitor was set 100%. IC_{50} values were determined by using the sigmoidal fitting method for plotting the steady-state levels of tubulin assembly (at 30 minutes after initiating the polymerization dynamic assay; excitation at 360 nm and emission at 420 nm) against drug concentrations and represent the concentrations of mHA1 (■), mHA6 (▲), mHA11 (▼), and colchicine (◆) for inhibition of the maximum tubulin polymerization level. Each point represents the mean value of 3 independent experiments.

To further determine whether the quantity and distribution of microtubule changes after treatment with these compounds, we conducted an immunofluorescent staining study. Under normal culture condition, CRL 5908 cells were grown in spindle morphology and microtubules were arrayed along the long axes in the cytoplasm (Fig. 6). However, 24 hours after treatment with mHA11 (similar results were obtained after treatment with mHA1 or mHA6), the 5,908 cells had shrunk, and the cell shape was changed from spindle to round, irregular, or multiangular. The long microtubule structure in cytoplasm was disrupted and the microtubule fluorescence intensity was significantly reduced, suggesting the decrease in contents of microtubule.

Docking study of HA14-1 analogs

The crystal structure of α/β-tubulin heterodimers in a complex with DAMA-colchicine reveals that colchicine binds at the interface of the α/β-tubulin heterodimer and inhibits the assembly of microtubules by preventing curved tubulin from adopting a straight structure. The results of our docking study show that mHA1, mHA6, and mHA11 could bind at the same site as colchicine on the tubulin protein. mHA1 and mHA6 adopt a similar binding mode, which is slightly different from that adopted by mHA11 (Fig. 7).

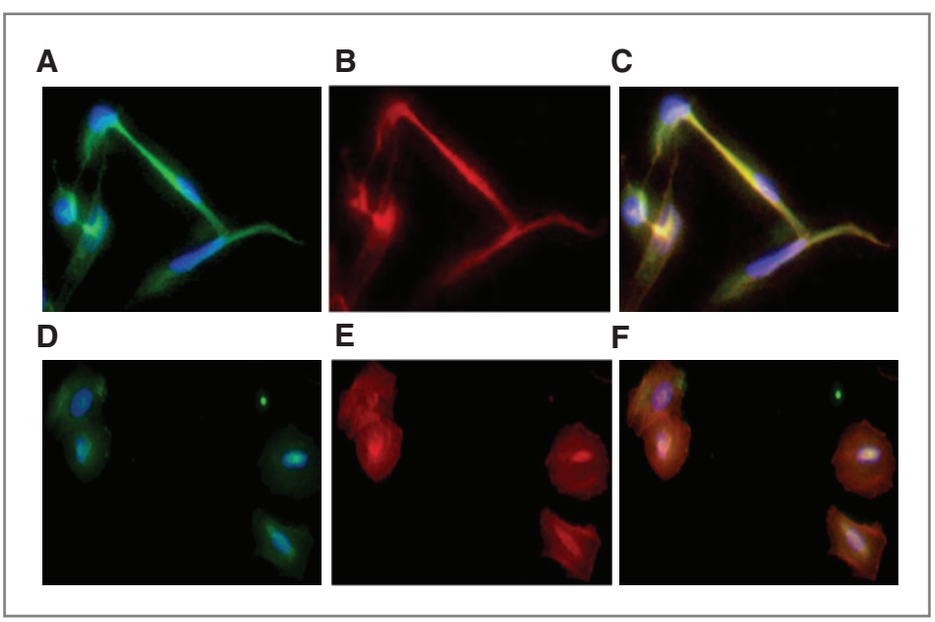

Figure 6. Effects of mHAs on cellular microtubules. Top, expression of microtubules (A), actin (B), and both microtubules and actin (C, merged image) in nontreated CRL 5908 lung cancer cells. Bottom, expression of microtubules (D), actin (E), and both microtubules and actin (F, merged image) in CRL 5908 cells 24 hours after treatment with 1 μmol/L mHAs. The result was representative of 3 independent experiments.

Published OnlineFirst May 10, 2013; DOI: 10.1158/1541-7786.MCR-12-0177

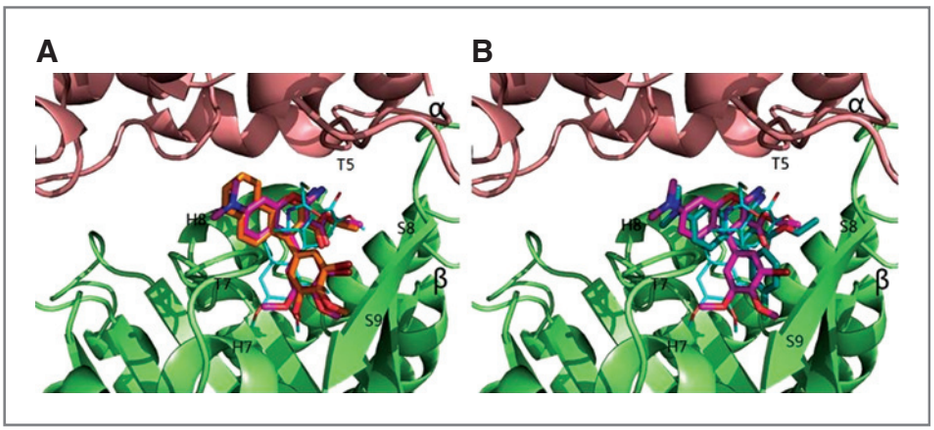

Figure 7. Comparison of the predicted binding models of mHA1, mHA6, and mHA 11 to the tubulin protein with that of DAMA-colchicine in the crystal structure. A, mHA1 and mHA6 bind to the colchicine-binding site in the same manner. B, the binding modes of mHA1 and mHA11 differ slightly. Carbon atoms in mHA1, mHA6, and mHA11 are shown as sticks; and DAMA-colchicine as lines. The carbon atoms are colored in magenta for mHA1, in orange for mHA6, in deep teal for mHA11, and in cyan for DAMA-colchicine. Nitrogen and oxygen atoms are colored in blue and red, respectively. These figures were rendered using Pymol.

Discussion

HA14-1, the first reported Bcl-2 inhibitor identified by our group, can potently induce apoptosis in a wide variety of human cancers (12, 18–21). At concentrations above 10 μmol/L, it also inhibits tubulin polymerization. We developed a series of HA14-1 analogs and identified a new class of 2-amino-4-phenyl-*4H*-chromene-3-carboxylate analogs: mHA1, mHA6, and mHA11 (Fig. 1). These analogs showed a more stable and more potent anticancer growth activity than did authentic HA14-1, with IC_{50} values of less than 1 μmol/L at 72 hours in the HL-60/Bcl-2 cell line; whereas the IC_{50} value for HA14-1 of was about 10 μmol/L. These new analogs also exhibited a mode of action that is different from that of HA14-1. HA14-1 is a fast-working agent: it induces reactive oxygen species (ROS) generation, cytochrome *c* release, and caspase-9/-3 activation (18, 22) within few hours after administration of treatment, which suggested that these responses are its main mechanism for killing tumor cells. Typical morphological changes associated with apoptotic cells, such as cell shrinkage, nuclear fragmentation, and chromatin condensation, occurred within 6 to 24 hours after treatment with HA14-1. However, these new analogs induced different types of morphological changes, including cell elongation, asymmetry and formation of long pseudopodia (Fig. 3A). All of these changes suggested that these new analogs may target microtubule functions, which is important for maintenance of cell shape and for cell division.

Our docking and protein-based binding studies provided further confirmed that these compounds bind at the same site as colchicine on the tubulin protein, causing disruption of tubulin polymerization (Figs. 4–7). Analysis of DNA content by flow cytometry indicated that cells were blocked in the G_2–M phase and this was accompanied with a decrease in mitotic cells and an increase in apoptotic cells (Table 1). The inductions of apoptosis in HL-60/Bcl-2 cells caused by these compounds (Fig. 2; Table 1) were confirmed by DNA fragmentation analyses (Fig. 3B). These novel compounds represent a new class of the emerging group of inhibitors of tubulin assembly that show promising anticancer activities and limited toxicity to normal bone marrow cells (Figs. 2–7).

Microtubules are important molecular targets for anticancer therapy because of their critical role in mitosis. During mitosis, the microtubules of the interphase cytoskeleton depolymerize, and the tubulin repolymerizes to form the mitotic spindle (4). The duplicated chromosomes are then located and attached to the spindle for separation. This procedure requires highly coordinated microtubule dynamics. Therefore, agents such as taxanes, vinca alkaloids, and epothilones, and our newly synthesized HA14-1 analogs that disrupt microtubule dynamics also cause the arrest of cell-cycle progression at mitosis and eventually lead to apoptosis (9, 23). Although many MIAs are actively used in the clinic against a wide variety of solid tumors and hematological malignancies, many limitations of currently approved agents are encountered, including variable sensitivity of different cancers, innate and acquired drug resistance, side effects of peripheral neuropathy and neutropenia, and poor solubility that necessitates their clinical use (4, 9). In addition to the development of overexpression of drug efflux pumps (24), mutations in the genes encoding α- and β-subunits of tubulin and differential expression of tubulin isotypes that reduce the binding of a drug to tubulin also contribute to MIA resistance (25, 26). Therefore, discovery of new MIAs such as our HA14-1 analogs may be helpful in overcoming these problems and might offer advantages over the current agents used for chemotherapy. In contrast to our mHA agents, which inhibit tubulin polymerization, paclitaxel enhances tubulin polymerization and does not compete with colchicine binding to tubulin (Figs. 4–6). These data provide evidence that our mHA agents exerted their antimicrotubule effects via different mechanisms, including differences in the sites of tubulin binding (Fig. 7). In addition, use of these MIAs in combination with other

existing therapeutics could reduce the required doses of individual drugs, thereby lessening their toxicities and providing another way to overcome the shortcomings of currently used therapeutics (3, 27–29).

Bcl-2 is a proto-oncogene that prevents cells from undergoing apoptosis in response to cytotoxic stimuli. HL-60/Bcl-2 cells have been stably transfected with the pZip-Bcl-2 plasmid and they express higher levels of Bcl-2 protein than HL-60/neo cells do. Many rediscovered drug development strategies aim to affect multiple targets in a parallel fashion because multitarget drugs have a lower prevalence and reduced ranges of side effects than high-affinity, single-target drugs. mHA compounds were derived from HA-14-1, a known Bcl-2 binder and inhibitor. At concentrations lower than 5 μmol/L, mHA compounds predominantly targeted microtubules. However, at concentrations around 5 μmol/L, these mHA agents were also able to bind to Bcl-2 and inhibit Bcl-2 from binding with apoptotic protein-derived probes (our unpublished data). The dual-target effects of these mHAs on both microtubule and Bcl-2, and their biological significance (such as whether this contributes to their lower cytotoxic effects on normal cells; Fig. 2), need to be investigated further.

In summary, we have developed a novel class of anti-microtubule agents that show promising antitumor activity. These new HA14-1 analogs inhibit tubulin polymerization, thereby inducing cell-cycle G_2–M arrest and apoptosis. The promising cytotoxic effects on cancer cells with IC_{50} value at nmol/L ranges, coupled with the minor cytotoxic effects on normal bone marrow cells, indicate that these new analogs have a good therapeutic window and that their further development as therapeutics for human use will be worthwhile.

Disclosure of Potential Conflicts of Interest

No potential conflicts of interest were disclosed.

Authors' Contributions

Conception and design: J. Xi, X. Zhu, G. Luo, R.C. Luo, Z. Huang, J. An
Development of methodology: J. Xi, X. Zhu, G. Luo, J. An
Acquisition of data (provided animals, acquired and managed patients, provided facilities, etc.): J. Xi, N. Huang, G. Wang
Analysis and interpretation of data (e.g., statistical analysis, biostatistics, computational analysis): J. Xi, X. Zhu, N. Huang, Y. Mao, X. Han, J. An
Writing, review, and/or revision of the manuscript: J. Xi, X. Zhu, N. Huang, R.C. Luo, Z. Huang, J. An
Administrative, technical, or material support (i.e., reporting or organizing data, constructing databases): Y. Mao, W. Tian, X. Han, R.C. Luo, J. An
Study supervision: G. Wang, R.C. Luo, Z. Huang, J. An

Grant Support

This work was partly supported by grants from the Connolly Endowment/Hendricks Fund and the LUNGevity Foundation.

The costs of publication of this article were defrayed in part by the payment of page charges. This article must therefore be hereby marked *advertisement* in accordance with 18 U.S.C. Section 1734 solely to indicate this fact.

Received March 27, 2012; revised March 20, 2013; accepted April 11, 2013; published OnlineFirst May 10, 2013.

References

1. Lopez-Fanarraga M, Avila J, Guasch A, Coll M, Zabala JC. Review: postchaperonin tubulin folding cofactors and their role in microtubule dynamics. J Struct Biol 2001;135:219–29.
2. Hall A. The cytoskeleton and cancer. Cancer Metastasis Rev 2009; 28:5–14.
3. Jordan MA, Wilson L. Microtubules as a target for anticancer drugs. Nat Rev Cancer 2004;4:253–65.
4. Risinger AL, Giles FJ, Mooberry SL. Microtubule dynamics as a target in oncology. Cancer Treat Rev 2009;35:255–61.
5. Mollinedo F, Gajate C. Microtubules, microtubule-interfering agents and apoptosis. Apoptosis 2003;8:413–50.
6. Zhou J, Giannakakou P. Targeting microtubules for cancer chemotherapy. Curr Med Chem Anticancer Agents 2005;5:65–71.
7. Dumontet C, Jordan MA. Microtubule-binding agents: a dynamic field of cancer therapeutics. Nat Revs Drug Discov 2010;9:790–803.
8. Carlson RO. New tubulin targeting agents currently in clinical development. Expert Opin Investig Drugs 2008;17:707–22.
9. Perez EA. Microtubule inhibitors: differentiating tubulin-inhibiting agents based on mechanisms of action, clinical activity, and resistance. Mol Cancer Ther 2009;8:2086–95.
10. Morris PG, Fornier MN. Microtubule active agents: beyond the taxane frontier. Clin Cancer Res 2008;14:7167–72.
11. Gascoigne KE, Taylor SS. How do anti-mitotic drugs kill cancer cells? J Cell Sci 2009;122:2579–85.
12. Wang JL, Liu D, Zhang ZJ, Shan S, Han X, Srinivasula SM, et al. Structure-based discovery of an organic compound that binds Bcl-2 protein and induces apoptosis of tumor cells. Proc Natl Acad Sci U S A 2000;97:7124–9.
13. An J, Chen Y, Huang Z. Critical upstream signals of cytochrome c release induced by a novel Bcl-2 inhibitor. J Biol Chem 2004; 279:19133–40.
14. Risinger AL, Westbrook CD, Encinas A, Mülbaier M, Schultes CM, Wawro S, et al. ELR510444, a novel microtubule disruptor with multiple mechanisms of action. J Pharmacol Exp Ther 2011;336: 652–60.
15. LaVallee TM, Burke PA, Swartz GM, Hamel E, Agoston GE, Shah J, et al. Significant antitumor activity in vivo following treatment with the microtubule agent ENMD-1198. Mol Cancer Ther 2008;7: 1472–82.
16. Ravelli RB, Gigant B, Curmi PA, Jourdain I, Lachkar S, Sobel A, et al. Insight into tubulin regulation from a complex with colchicine and a stathmin-like domain. Nature 2004;428:198–202.
17. Kitazumi I, Tsukahara M. Regulation of DNA fragmentation: the role of caspases and phosphorylation. FEBS J 2011;278:427–41.
18. An J, Nie A, Chervin A, Ducoff HS, Huang Z. Overcoming the radioresistance of prostate cancer cells with a novel Bcl-2 inhibitor. Oncogene 2007;26:652–61.
19. Manero F, Gautier F, Gallenne T, Cauquil N, Grée D, Cartron PF, et al. The small organic compound HA14-1 prevents Bcl-2 interaction with Bax to sensitize malignant glioma cells to induction of cell death. Cancer Res 2006;66:2757–64.
20. Sinicrope FA, Penington RC, Tang XM. Tumor necrosis factor-related apoptosis-inducing ligand-induced apoptosis is inhibited by Bcl-2 but restored by the small molecule Bcl-2 inhibitor, HA 14-1, in human colon cancer cells. Clin Cancer Res 2004;10:8284–92.
21. Campàs C, Cosialls AM, Barragán M, Iglesias-Serret D, Santidrián AF, Coll-Mulet L, et al. Bcl-2 inhibitors induce apoptosis in chronic lymphocytic leukemia cells. Exp Hematol 2006;34:1663–9.
22. Hermanson D, Addo SN, Bajer AA, Marchant JS, Das SG, Srinivasan B, et al. Dual mechanisms of sHA 14-1 in inducing cell death through endoplasmic reticulum and mitochondria. Mol Pharmacol 2009;76: 667–78.
23. Yue QX, Liu X, Guo DA. Microtubule-binding natural products for cancer therapy. Planta Med 2010;76:1037–43.
24. Fojo AT, Menefee M. Microtubule targeting agents: basic mechanisms of multidrug resistance (MDR). Semin Oncol 2005;32:S3–8.

Published OnlineFirst May 10, 2013; DOI: 10.1158/1541-7786.MCR-12-0177

25. Loganzo F, Hari M, Annable T, Tan X, Morilla DB, Musto S, et al. Cells resistant to HTI-286 do not overexpress P-glycoprotein but have reduced drug accumulation and a point mutation in alpha-tubulin. Mol Cancer Ther 2004;3:1319–27.
26. Kanakkanthara A, Wilmes A, O'Brate A, Escuin D, Chan A, Gjyrezi A, et al. Peloruside- and laulimalide-resistant human ovarian carcinoma cells have betaI-tubulin mutations and altered expression of betaII- and betaIII-tubulin isotypes. Mol Cancer Ther 2011;10:1419–29.
27. Wilmes A, O'Sullivan D, Chan A, Chandrahasen C, Paterson I, Northcote PT, et al. Synergistic interactions between peloruside A and other microtubule-stabilizing and destabilizing agents in cultured human ovarian carcinoma cells and murine T cells. Cancer Chemother Pharmacol 2011;68:117–26.
28. Owonikoko TK, Ramalingam SS, Kanterewicz B, Balius TE, Belani CP, Hershberger PA. Vorinostat increases carboplatin and paclitaxel activity in non-small-cell lung cancer cells. Int J Cancer 2010;126:743–55.
29. Yardley DA, Raefsky E, Castillo R, Lahiry A, Locicero R, Thompson D, et al. Phase II study of neoadjuvant weekly nab-Paclitaxel and Carboplatin, with bevacizumab and trastuzumab, as treatment for women with locally advanced HER2(+) breast cancer. Clin Breast Cancer 2011;11:297–305.

AACR American Association for Cancer Research

Molecular Cancer Research

Development of a Novel Class of Tubulin Inhibitors with Promising Anticancer Activities

Jingle Xi, Xuejun Zhu, Yongmei Feng, et al.

Mol Cancer Res 2013;11:856-864. Published OnlineFirst May 10, 2013.